Combined Magnetic Nanoparticle-based MicroRNA and Hyperthermia Therapy to Enhance Apoptosis in Brain Cancer Cells

Perry T. Yin, Birju P. Shah, and Ki-Bum Lee*

In recent years, mild hyperthermia (40–45 °C) has been increasingly investigated as an adjuvant that can effectively sensitize tumors to chemotherapy and radiotherapy as well as induce apoptosis.[1] In particular, magnetic hyperthermia, wherein the exposure of magnetic nanoparticles (MNPs) to an alternating magnetic field (AMF) results in the induction of hyperthermia via Neel and Brownian relaxation, represents an attractive approach for the selective heating of tumors while sparing surrounding healthy tissues.[2] However, the treatment of tumors with magnetic hyperthermia results in a number of molecular effects including a sharp increase in the synthesis of heat shock proteins (HSPs), whose fundamental function is to protect cellular proteins from degradation. It has been reported that these effects occur through numerous signaling pathways involved in therapeutic resistance including the activation of DNA repair mechanisms (via the BRCA family)[3] and the inhibition of apoptosis (via the Akt/PI3K pathway).[4,5] As such, HSP expression following magnetic hyperthermia significantly hinders MNP-mediated apoptosis in cancer cells. For instance, it has been demonstrated that the activation of HSPs preserves cancer cell viability and can impart cancer cells with resistance to chemotherapy and radiotherapy.[6]

A number of therapeutics are currently being investigated for their ability to target HSP-related pathways. For example, the proteasome inhibitor, bortezimab, targets the NF-kB pathway, which is in part regulated by HSP70 and HSP90.[7] There are also agents directed at the HSP90 and mTOR/HIF pathways including the inhibitor geldanamycin.[8] For instance, Yoo et al. developed resistance-free apoptosis-inducing magnetic nanoparticles (RAIN) composed of MNPs that release geldanamycin to inhibit HSP90 and induce magnetic hyperthermia upon exposure to an

AMF.[9] While promising, each individual of the HSP family (e.g., HSP27, HSP70, HSP72, HSP90) has numerous subsequent targets whose pathways have significant degeneracy.[10] Therefore, to maximize the therapeutic potential of magnetic hyperthermia for the treatment of cancer, there is a clear need to simultaneously target the multiple key downstream effectors of HSPs that promote cell survival and inhibit apoptosis following treatment.

Herein, we report the novel application of highly magnetic zinc-doped iron oxide nanoparticles ($ZnFe_2O_4$) for the dual purpose of delivering a microRNA (miRNA) that targets multiple downstream pathways modulated by HSPs and inducing magnetic hyperthermia to enhance the treatment of cancer cells (**Figure 1**a). Specifically, in this study, glioblastoma multiforme (GBM) brain cancer cells were used as a model system. miRNAs are small endogenous noncoding RNA molecules that interact with target messenger RNAs (mRNAs) to down-regulate or inhibit translation. The function of miRNAs in cancer formation and treatment is well established.[11] However, the unique feature that makes miRNA particularly suitable to combine with magnetic hyperthermia is their ability to have multiple, possibly hundreds of, targets.[12] Moreover, these targets are often on the same or similar pathways. Therefore, the delivery of a single miRNA can potentially have a greater, more cumulative effect on HSPs and their downstream effectors than delivering other types of therapeutic molecules such as small interfering RNA (siRNA) molecules or drugs, which can only modulate single HSP-related targets.[13] To this end, we are interested in delivering lethal-7a miRNA (let-7a), which is known to be a tumor suppressor that inhibits malignant growth by targeting factors such as the BRCA family, RAS, IGF1R, and c-Myc, which overlap with a number of key downstream effectors of HSPs.[14] Moreover, let-7a has been reported to be down-regulated in a number of cancer types including cancers of the prostate, breast, and brain, where let-7a is decreased by over 3-fold compared to healthy surrounding tissue.[15] As such, we hypothesized that the MNP-mediated delivery of let-7a should act synergistically with magnetic hyperthermia to enhance hyperthermia-mediated apoptosis by targeting multiple key HSP-related pathways including DNA repair and cell survival (via IGF1R and RAS) mechanisms.

For the MNP-based combined miRNA and magnetic hyperthermia therapy, we utilized zinc doped iron oxide

P. T. Yin, Prof. K.-B. Lee
Department of Biomedical Engineering
Rutgers, The State University of New Jersey
599 Taylor Road, Piscataway, NJ 08854, USA
E-mail: kblee@rutgers.edu

B. P. Shah, Prof. K.-B. Lee
Department of Chemistry and Chemical Biology
Rutgers, The State University of New Jersey
610 Taylor Road, Piscataway, NJ 08854, USA
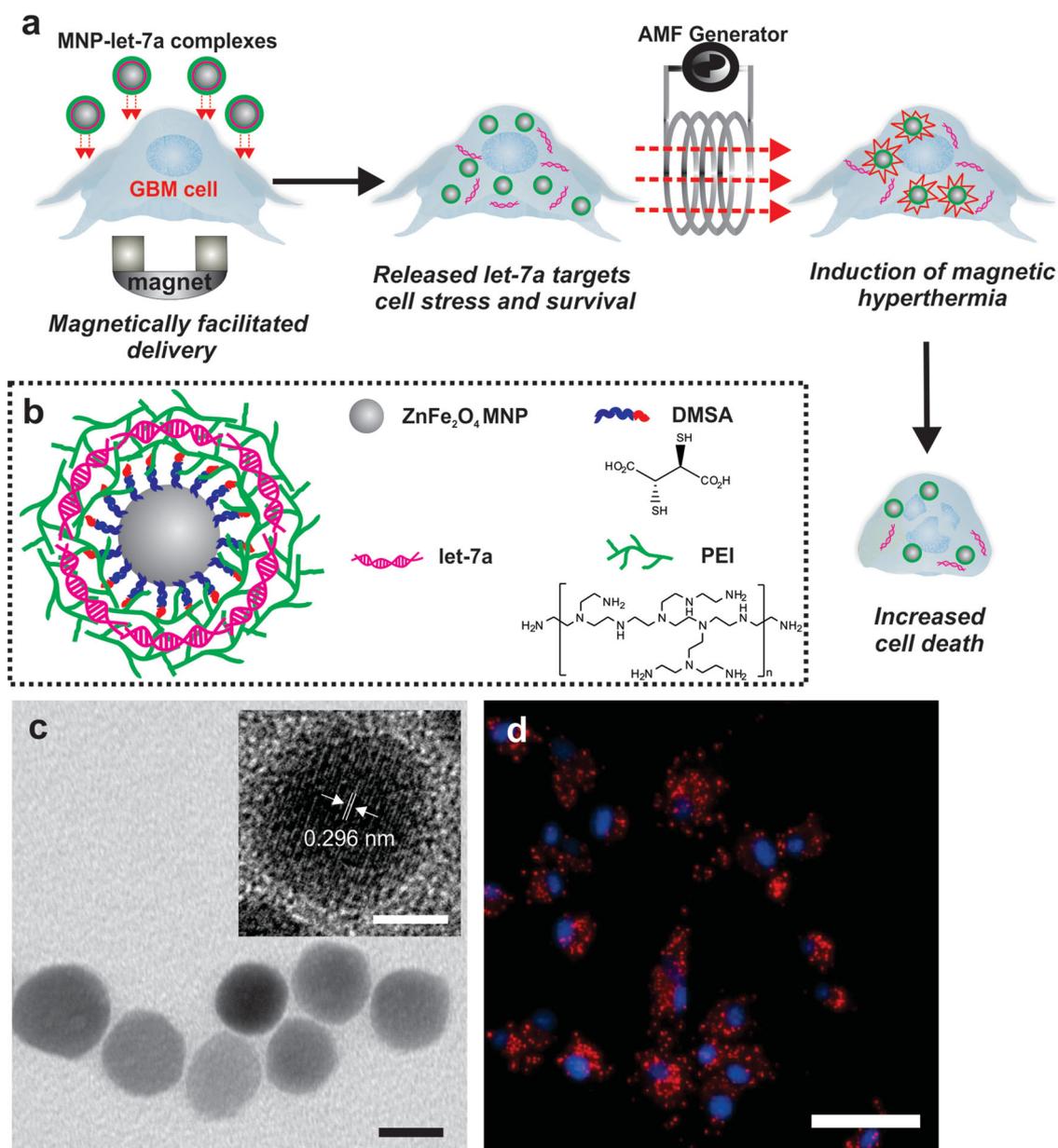
DOI: 10.1002/smll.201400963

Figure 1. Magnetic nanoparticle-based microRNA and hyperthermia therapy to enhance the treatment brain cancer. a) MNP complexes are first delivered to GBM cells, which is enhanced by magnetofection. Once inside the cell, let-7a miRNA is released thereby targeting downstream effectors of HSPs. This sensitizes the cancer cells to subsequent magnetic hyperthermia enhancing apoptosis. b) MNPs will be complexed with let-7a miRNA using 10 kDa branched PEI via a layer-by-layer approach. c) TEM image of the MNPs (scale bar = 20 nm). Inset: High resolution TEM image of the MNPs showing the lattice fringes (scale bar = 10 nm). d) U87-EGFRvIII GBM cells readily uptake MNPs complexed with Cy3-labeled scrambled miRNA following magnetofection (scale bar = 50 μm). Blue = hoescht stained nuclei, red = cy3-labeled scrambled miRNA.

($ZnFe_2O_4$) nanoparticles. These MNPs have previously been shown to have a significantly higher magnetic susceptibility and hence, can afford improved magnetic properties while requiring a much lower dose when compared to conventional Fe_2O_3 or Fe_3O_4 nanoparticles.[16] As such, we first synthesized $ZnFe_2O_4$ MNPs with a doping percentage of $(Zn_{0.4}Fe_{0.6})$ Fe_2O_4 via the thermal decomposition of a mixture of metal precursors (zinc chloride, ferrous chloride, and ferric acetylacetonate) in the presence of oleic acid using a previously reported protocol that was modified by our group.[16,17] The resulting highly monodisperse and hydrophobic $ZnFe_2O_4$ MNPs were then made water-soluble via ligand exchange with 2,3-dimercaptosuccinic acid (DMSA).[18] Transmission electron microscopy (TEM) analysis revealed that the overall diameter of the $ZnFe_2O_4$ MNPs was 22.92 ± 3.7 nm (Figure 1c). A high-resolution TEM image shows the monocrystalline structure of the MNPs with a lattice fringe that was measured to be 0.296 nm (Inset of Figure 1c), which is characteristic of the (220) planes of the spinel and is in agreement with previous reports.[16,17] In terms of the water soluble MNPs, it was found that the DMSA coated MNPs had a hydrodynamic size of 30.1 ± 2.8 nm (polydispersity index [PDI] = 0.192) as measured by dynamic light scattering (DLS) and a zeta potential of –23.3 ± 1.3 mV. Moreover, with regard to their

magnetic properties, the MNPs were characterized by a specific absorption rate (SAR) of 341 W/g, which was determined using an AMF with an amplitude of 5 kA/m and a frequency of 225 kHz. This SAR is consistent with data reported in the literature for similar $ZnFe_2O_4$ MNPs.[19] In comparison, we found that conventional Fe_3O_4 MNPs (7 nm diameter) have a SAR of 28.46 W/g, which is also in agreement with values that have been reported (10–40 W/g).[20] As such, our monodisperse water soluble $ZnFe_2O_4$ MNPs are characterized by expectedly superior magnetic properties thereby allowing for the use of significantly lower doses when compared to conventional MNPs.

To prepare the aforementioned $ZnFe_2O_4$ MNPs for miRNA delivery, the negatively charged water-soluble MNPs were coated with a 10 kDa branched cationic polymer, polyethyleneimine (PEI), which affords the MNPs with an overall positive charge. PEI is a polymer that is partially protonated under physiological conditions, thus allowing for the formation of complexes in the presence of nucleic acids. Previous studies have shown that a direct relationship exists between the molecular weight of PEI and cytotoxicity.[21] Therefore, to minimize cytotoxicity while maximizing transfection efficiency we used 10 kDa branched PEI (Figure S1a, Supporting Information). In particular, to deliver miRNAs efficiently using our MNPs, we developed a two-step layer-by-layer process (Figure 1b). First, the PEI-coated MNPs (1 μg/mL) were incubated with miRNA in an 80 mm NaCl solution. Afterwards, an outer coat of PEI was added to provide additional protection for the miRNA as well as to facilitate cell uptake and endosomal escape. We observed that the size of the MNP complexes increased to a final diameter of 76.91 ± 11 nm (PDI = 0.242) for the layer-by-layer MNP-PEI/miRNA/PEI complex and had a positive zeta potential of +23.7 ± 1.7 mV. Moreover, a reversal of the zeta potential was observed after the deposition of each layer (Figure S1b, Supporting Information). A more detailed description of the optimization process for MNP complex formation can be found in the Supporting Information (Figure S1).

To assess the efficiency of cellular uptake, we performed fluorescence microscopy on GBM cells (U87-EGFRvIII) that were transfected with MNP-PEI/miRNA/PEI complexes (Figure 1d). In this case, the MNP complexes were assembled using 100 nm Cy3-labeled scrambled precursor miRNA (Ambion) and delivery was enhanced by magnetofection, a well-established method that allows for the rapid accumulation of MNPs and their payloads upon exposure to an external magnetic field.[17,22] Twenty-four hours after transfection, we visualized and quantified the efficiency of uptake. We found that that the GBM cells were able to efficiently uptake the MNP-PEI/Cy3-miRNA/PEI complexes (98% efficiency). Moreover, compared to commercially available transfection agents (X-tremeGENE), the fluorescence intensity of Cy3-miRNA uptaken after magnetofection using our layer-by-layer MNP complexes was significantly greater (Figure S2, Supporting Information). To further confirm MNP uptake, cross-sectional cellular images were obtained using TEM (Figure S3, Supporting Information). Finally, in contrast to other cationic transfection methods, which can result in low cell viabilities,[23] the MNP complexes and

the process of magnetofection caused little to no cell death (92% cell viability) owing to the much lower concentration and shorter time of incubation that is necessary. As such, this demonstrates that these complexes can be used for extended incubation and downstream applications such as magnetic hyperthermia or imaging (Figure S4a, Supporting Information).

As mentioned previously, let-7a is known to target a number of genes involved in cell survival (PI3K via IGF1R)[4,5] and proliferation (RAS)[24] (**Figure 2**a). To confirm this in GBM, we first delivered 70-nucleotide precursor let-7a miRNA (100 nm) to U87-EGFRvIII GBM cells using our optimized MNP-based delivery conditions and quantified the mRNA expression levels of selected let-7a targets. Specifically, using quantitative PCR (qPCR) measurements made from total RNA, we observed at least 40% down-regulation ($p < 0.05$) of all target gene transcripts (KRAS, NRAS, c-MYC, and IGF1R) relative to U87-EGFRvIII cells treated with scrambled miRNA (100 nm) as delivered by our MNPs (Figure 2b; Figure S5, Supporting Information). This is also supported by Lee et al., who reported that let-7 can inhibit proliferation in GBM cells (e.g., U251 and U87) via the down regulation of NRAS and KRAS.[25] These results not only confirm that let-7a targets the desired genes in GBM cells but also that the function and target-specificity of let-7a is retained upon cellular uptake/endosomal escape.

Next, to induce apoptosis and evaluate the therapeutic potential of let-7a, we modulated intracellular levels of this miRNA. We observed that 48 h after the MNP-mediated delivery of let-7a, GBM cell viability decreased significantly compared to scrambled miRNA controls in a dose-dependent fashion (Figure 2c). Using 100 nm miRNA as the optimal concentration for the remainder of the studies, apoptosis levels in the GBM cells were evaluated using Annexin-V/propidium iodide staining and qPCR of caspase-3 expression. In particular, FACS analysis of Annexin-V/propidium iodide stained cells demonstrated that significantly more cells underwent apoptosis after treatment with let-7a (Figure 2d) compared to scrambled miRNA controls. Similarly, the expression of caspase-3 was up regulated by 30% ($p < 0.05$) after treatment with let-7a as compared to scrambled miRNA control (Figure 2e).

In terms of the effect that let-7a delivery has on key signaling pathways, we observed that the delivery of let-7a to GBM cells resulted in a significant decrease in the expression of PI3K (56% decrease, $p < 0.05$), which typically promotes cell survival and inhibits apoptosis.[26] As PI3K is downstream of let-7a targets including RAS and IGF1R (Figure 2a),[27] this result suggests that let-7a induces apoptosis in GBM cells via the targeting of RAS and IGF1R. Finally, we investigated the efficacy of let-7a delivery to other GBM cell lines (U87-WT, U87-EGFR) as well as normal brain cells (astrocytes) (Figure S4b, Supporting Information). We found that let-7a appears to be most effective in U87-EGFRvIII cells compared to U87-WT and U87-EGFR cells possibly because the U87-EGFRvIII cell line overexpresses EGFRvIII, which is upstream of PI3K.[24] Moreover, we observed that let-7a does not induce cytotoxicity in normal brain cells (astrocytes), which is expected as non-cancer cells should have much
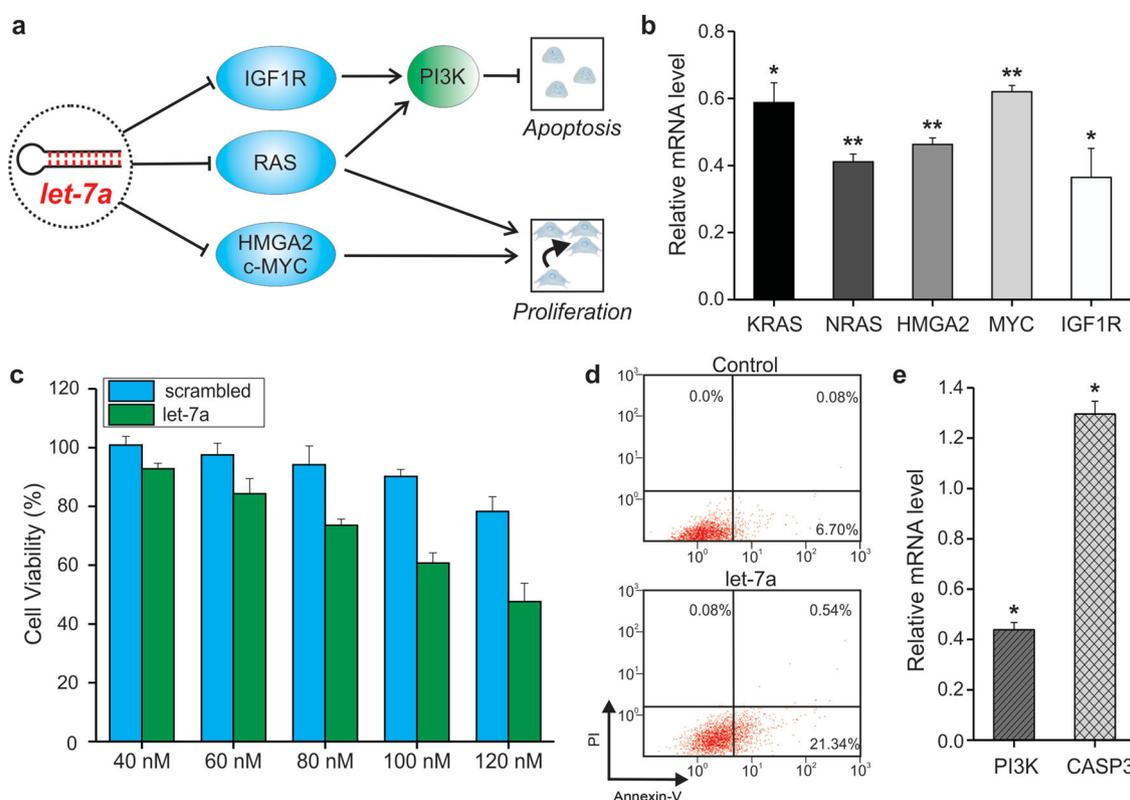
Figure 2. Magnetic nanoparticle-based let-7a delivery. a) The delivery of let-7a can inhibit targets such as IGF1R, RAS, HMGA2, and c-MYC, which typically promote proliferation and cell survival while inhibiting apoptosis. b) The delivery of let-7a to U87-EGFRvIII GBM cells significantly down-regulates expected targets of let-7a compared to scrambled miRNA controls as determined by qPCR (*$p < 0.05$, **$p < 0.01$). c) Cell viability as quantified by MTS assay 48 h after initial transfection with let-7a. Samples were normalized to untreated controls. d) FACS analysis of Annexin-V and propidium iodide stained cells. e) qPCR of downstream targets of let-7a compared to scrambled miRNA controls (*$p < 0.05$).

higher endogenous levels of let-7a compared to brain cancer cells.[15]

To evaluate the ability of our MNP complexes to induce magnetic hyperthermia, we delivered MNP-PEI (10 μg/mL, Supporting Information Figure S6a) to U87-EGFRvIII cells. Twenty-four hours after treatment, the MNP-PEI transfected cells were trypsinized and exposed to an AMF (5 kA/m, 225 kHz). We found that the therapeutic effect of magnetic hyperthermia was dose-dependent with the lowest cell viability (63.14%) being achieved after 45 min of exposure to an AMF (**Figure 3**a). Moreover, an increase in the level of apoptosis was observed as quantified via Annexin-V/PI staining (Figure 3b) and the mRNA expression level of caspase-3 (twofold increase) when compared to control cells transfected with MNPs but not exposed to an AMF (Figure 3c). Finally, to determine the approximate temperature that was achieved at this MNP concentration, we monitored the temperature of the solution containing GBM cells that had been transfected with 10 μg/mL of MNPs using a fiber optic temperature probe. We observed that after 45 min of exposure to an AMF, an approximate temperature of 44.1 °C was reached (Figure 3d).

To study the effect that hyperthermia has on the expression of HSPs and the activation of their downstream effectors, we confirmed that magnetic hyperthermia significantly increases the expression of HSPs including HSP70 (4.1-fold, $p < 0.005$), HSP72 (5.4-fold, $p < 0.001$), and HSP90 (2.9-fold,

$p < 0.05$), which have all been implicated in cancer progression and chemoresistance (Figure 3c).[28,29] Moreover, downstream effectors of these HSPs such as IGF1R, RAS, and PI3K, which are well-known to inhibit apoptosis and promote cell survival, are also significantly activated ($p < 0.01$) when compared to controls that have not been exposed to magnetic hyperthermia (Figure 3e; Figure S7, Supporting Information). As such, while MNP-mediated magnetic hyperthermia does induce significant toxicity in GBM cells, the activation of pathways that promote cell survival and inhibit apoptosis is also apparent suggesting that the inhibition of these multiple key downstream effectors can potentially improve the therapeutic effects of MNP-mediated magnetic hyperthermia.

To test the hypothesis that the MNP-based combined miRNA and magnetic hyperthermia therapy would enhance the therapeutic effects of let-7a delivery or magnetic hyperthermia alone, we delivered MNP-PEI/miRNA/PEI complexes to U87-EGFRvIII cells. Twenty-four hours after treatment, the cells were trypsinized and exposed to an AMF. This treatment sequence, as depicted in **Figure 4**a, was chosen because an independent study demonstrated it to be the optimal treatment time for combined therapy (Figure S6b, Supporting Information). This is expected as the maximal effects of magnetic hyperthermia are typically seen within 24 hours whereas miRNAs such as let-7a act over 48–72 h. Overall, combined MNP-based let-7a delivery and magnetic
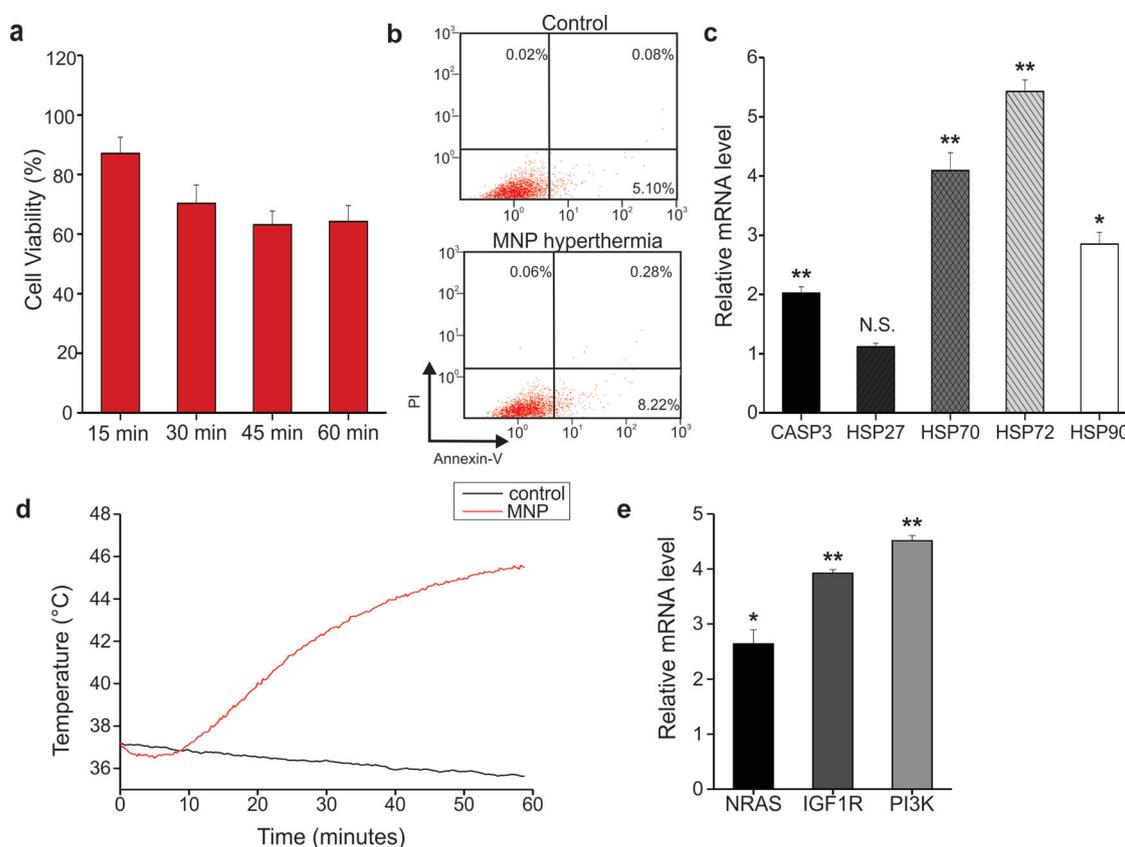
Figure 3. Magnetic nanoparticle-based magnetic hyperthermia. a) MTS assay following the induction of magnetic hyperthermia (10 μg/mL MNP) in U87-EGFRvIII GBM cells. Conditions were assayed 48 hours after transfection and normalized to MNP controls (without exposure to AMF). b) FACS analysis of Annexin-V and propidium iodide stained cells with and without treatment. c) qPCR illustrates that, following magnetic hyperthermia, caspase-3 is significantly up regulated as are HSPs. Results were normalized to MNP controls without magnetic hyperthermia (*$p < 0.05$, **$p < 0.01$, N.S. = no significance). d) The temperature of the solution was monitored using a fiber optic temperature probe (Lumasense) over the course of magnetic hyperthermia. Control consisted of the same conditions but without MNPs. e) qPCR shows up regulation of let-7a targets following magnetic hyperthermia. Again, results were normalized to MNP controls in the absence of magnetic hyperthermia (*$p < 0.01$, **$p < 0.001$).

hyperthermia exhibited an additive effect resulting in a cell viability as low as 34% (Figure 4b), which is significantly lower than either let-7a treatment (69.8%, $p < 0.01$) or magnetic hyperthermia alone (63.14%, $p < 0.05$). Moreover, a significant increase in apoptosis levels was observed as quantified via Annexin-V/PI staining (Figure 4c) and the mRNA expression of caspase-3 (80% increase) when compared to either let-7a treatment or magnetic hyperthermia alone (Figure 4d). To further demonstrate the potential of our combined MNP-based let-7a delivery and magnetic hyperthermia therapy, we utilized a tumor spheroid monoculture assay as an intermediate between in vitro monolayer-based models and future in vivo studies. Specifically, unlike classical monolayer-based models, tumor spheroid models are able to mirror the three-dimensional (3D) context of in vivo tumors to a high degree and can provide more therapeutically relevant results.[30] In particular, we observed that upon exposure to combined therapy using the same conditions as those used in monolayer cell cultures, we saw a similar additive effect resulting in tumor spheroid cell viability as low as 47% (Figure S9, Supporting Information). As expected of a 3D environment, although still effective, combined therapy was not as effective as in monolayer cultures across all conditions (e.g., let-7a alone, magnetic hyperthermia alone, and

combined therapy). Finally, as a preliminary in vivo study, we performed a biodistribution study wherein MNP complexes (25 and 50 mg MNP/kg of body weight) functionalized with poly(ethylene glycol) (PEG; molecular weight = 2000 g/mol) and targeted via anti-CD44 antibodies were injected (tail-vein injection) into nu/nu mice implanted with subcutaneous SUM159 xenografts. We found that the animals tolerated both doses well and that the MNPs were able to localize/target the tumors within one week of injection (Figures S10, Supporting Information). While more detailed in vivo studies remain to be performed, our findings taken together with previous evidence demonstrating the effectiveness of let-7 alone in vivo[25] and magnetic hyperthermia alone in vivo[2,31] suggests that combined MNP-based let-7a delivery and magnetic hyperthermia will be able to act as an effective treatment in vivo.

Finally, to examine the molecular mechanisms by which MNP-based combined let-7 and magnetic hyperthermia therapy can increase cell death in GBM cells, we investigated its target genes focusing on those related to HSPs as well as cell survival and proliferation (Figure 4d; Figure S8, Supporting Information). Specifically, we observed that PI3K expression was significantly down regulated (23% decrease, $p < 0.001$) whereas caspase-3 was significantly up regulated
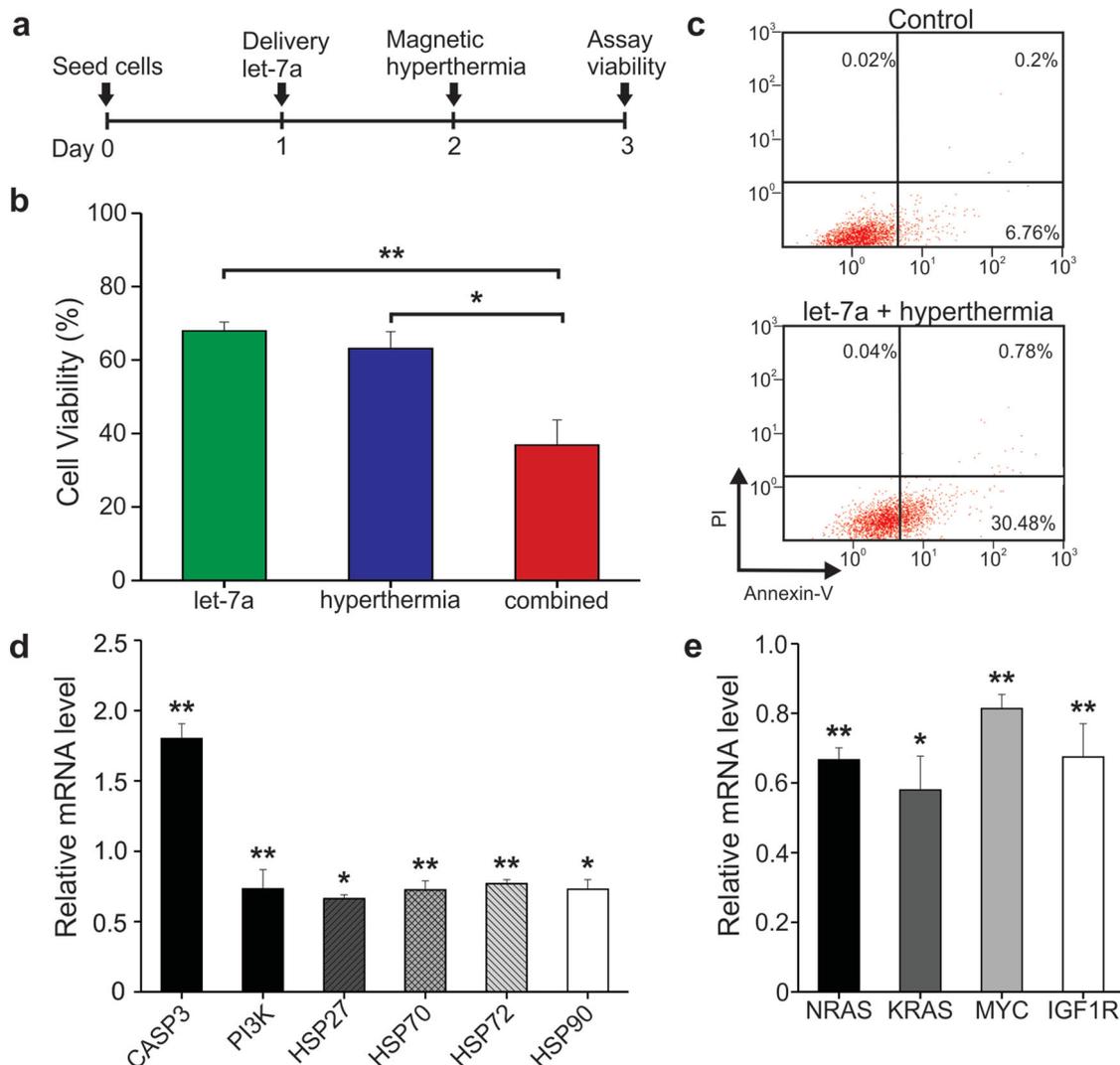
Figure 4. Combined magnetic nanoparticle-based let-7a delivery and magnetic hyperthermia therapy. a) Timeline of combined treatment. b) Cell viability following combined let-7a delivery and magnetic hyperthermia as quantified by MTS assay (*$p < 0.05$, **$p < 0.01$). c) FACS analysis of combination treated cells compared to controls. d) Combined let-7a delivery and magnetic hyperthermia results in up regulation of caspase-3 and a decrease in PI3K as well as HSPs as determined by qPCR (*$p < 0.05$, **$p < 0.01$). e) qPCR analysis of let-7a targets following combined therapy (*$p < 0.05$, **$p < 0.01$). qPCR results were normalized to MNP-PEI/miRNA/PEI complex controls delivering scrambled miRNA without exposure to magnetic hyperthermia.

(80% increase, $p < 0.001$) when magnetic hyperthermia was combined with let-7a delivery (Figure 4d). Moreover, the expression of HSPs was also significantly down regulated (>20%, $p < 0.02$) when compared to magnetic hyperthermia treated control cells. In terms of let-7a targets, the expression of RAS, IGF1R, and MYC were down regulated significantly after exposure to combined therapy (Figure 4e; Figures S8, Supporting Information). These results suggest that the down regulation of pathways including IGF1R and RAS, which directly activate PI3K,[27] by let-7a may lead to a greater increase in caspase-3 mediated apoptosis than would otherwise be possible with magnetic hyperthermia or let-7a delivery alone. Moreover, it has been shown that the inhibition of PI3K can also down regulate HSPs,[32] which is supported by the down regulation of HSP that is observed in our results (Figure 4d), further pushing GBM cells towards apoptosis following combined therapy. Together, these results

suggest that the MNP-based combination of let-7a delivery followed by magnetic hyperthermia may significantly enhance the treatment of GBM.

In summary, we have successfully demonstrated the effective MNP-based delivery of miRNA to cancer cells as well as the novel combined MNP-based miRNA and magnetic hyperthermia therapy to enhance apoptosis in cancer cells. As mentioned previously, to maximize the therapeutic effects of hyperthermia, a number of therapeutics have been developed to target HSP-mediated pathways including the HSP70 and HSP90 inhibitor, bortezimab[7] and geldanamycin, which targets HSP90.[8] While promising, each individual of the HSP family (e.g., HSP27, HSP70, HSP72, HSP90) has numerous subsequent targets.[10] As such, in this study we sought to deliver a miRNA (let-7a), which simultaneously targets multiple key downstream effectors of HSPs on a MNP platform that also acts as an excellent magnetic hyperthermia

agent to enhance apoptosis in brain cancer cells. The results indicate that combined MNP-based let-7a delivery and magnetic hyperthermia showed an additive effect resulting in significantly more apoptosis in brain cancer cells than either let-7a treatment or magnetic hyperthermia alone. Moreover, our results suggest that the targeting of pathways such as IGF1R and RAS by let-7a may lead to an increase in caspase-3 mediated apoptosis. Finally, besides enhancing the effects of magnetic hyperthermia, combined MNP-based let-7a delivery and magnetic hyperthermia can also offer a number of other advantages. First, the use of MNPs allows for enhancement of transfection using magnetofection as well as magnetic targeting. Second, treatment can potentially be monitored via magnetic resonance imaging (MRI) owing to the use of MNPs. Finally, we believe this treatment strategy can enhance the therapeutic potential of magnetic hyperthermia and by choosing cancer-specific miRNAs, can even be applied to enhance the treatment of other cancers and cancer stem cells including, but not limited to, breast and prostate cancers. In the future, we plan to improve targeting and biocompability by the addition of targeting ligands (e.g., iRGD) and polyethylene glycol (PEG), respectively.

Supporting Information

Supporting Information is available from the Wiley Online Library or from the author.

Acknowledgements

[1] P. Wust, B. Hildebrandt, G. Sreenivasa, B. Rau, J. Gellermann, H. Riess, R. Felix, P. M. Schlag, *Lancet Oncol.* **2002**, *3*, 487–497.

[2] C. S. Kumar, F. Mohammad, *Adv. Drug Delivery Rev.* **2011**, *63*, 789–808.

[3] M. Landriscina, M. R. Amoroso, A. Piscazzi, F. Esposito, *Gynecol. Oncol.* **2010**, *117*, 177–182.

[4] C. Garrido, E. Solary, *Cell Death Differ.* **2003**, *10*, 619–620.

[5] S. Takayama, J. C. Reed, S. Homma, *Oncogene* **2003**, *22*, 9041–9047.

[6] C. Jolly, R. I. Morimoto, *J. Natl. Cancer I* **2000**, *92*, 1564–1572.

[7] E. G. Minnnaugh, W. P. Xu, M. Vos, X. T. Yuan, J. S. Isaacs, K. S. Bisht, D. Gius, L. Neckers, *Mol. Cancer Ther.* **2004**, *3*, 551–566.

[8] Y. Miyata, *Curr. Pharm. Design* **2005**, *11*, 1131–1138.

[9] D. Yoo, H. Jeong, S. H. Noh, J. H. Lee, J. Cheon, *Angew. Chem.* **2013**, *52*, 13047–13051.

[10] D. R. Ciocca, S. K. Calderwood, *Cell Stress Chaperones* **2005**, *10*, 86–103.

[11] G. A. Calin, C. M. Croce, *Nat. Rev. Cancer* **2006**, *6*, 857–66.

[12] D. P. Bartel, *Cell* **2009**, *136*, 215–233.

[13] A. G. Bader, D. Brown, M. Winkler, *Cancer Res.* **2010**, *70*, 7027–7030.

[14] S. Roush, F. J. Slack, *Trends Cell Biol.* **2008**, *18*, 505–516.

[15] I. Lavon, D. Zrihan, A. Granit, O. Einstein, N. Fainstein, M. A. Cohen, M. A. Cohen, B. Zelikovitch, Y. Shoshan, S. Spektor, B. E. Reubinoff, Y. Felig, O. Gerlitz, T. Ben-Hur, Y. Smith, T. Siegal, *J. Neuro-Oncol.* **2010**, *12*, 422–433.

[16] J. T. Jang, H. Nah, J. H. Lee, S. H. Moon, M. G. Kim, J. Cheon, *Angew. Chem. Int. Ed.* **2009**, *48*, 1234–1238.

[17] B. Shah, P. T. Yin, S. Ghoshal, K. B. Lee, *Angew. Chem. Int. Ed.* **2013**, *52*, 6190–6195.

[18] S. T. Guo, Y. Y. Huang, Q. A. Jiang, Y. Sun, L. D. Deng, Z. C. Liang, Q. A. Du, J. F. Xing, Y. L. Zhao, P. C. Wang, A. J. Dong, X. J. Liang, *ACS Nano* **2010**, *4*, 5505–5511.

[19] P. M. Zelis, G. A. Pasquevich, S. J. Stewart, M. B. F. van Raap, J. Aphesteguy, I. J. Bruvera, C. Laborde, B. Pianciola, S. Jacobo, F. H. Sanchez, *J. Phys. D Appl. Phys.* **2013**, *46*, 125006.

[20] P. Drake, H. J. Cho, P. S. Shih, C. H. Kao, K. F. Lee, C. H. Kuo, X. Z. Lin, Y. J. Lin, *J. Mater. Chem.* **2007**, *17*, 4914–4918.

[21] S. Werth, B. Urban-Klein, L. Dai, S. Hobel, M. Grzelinski, U. Bakowsky, F. Czubayko, A. Aigner, *J. Controlled Release* **2006**, *112*, 257–270.

[22] C. Plank, O. Zelphati, O. Mykhaylyk, *Adv. Drug Delivery Rev.* **2011**, *63*, 1300–1331.

[23] H. Lv, S. Zhang, B. Wang, S. Cui, J. Yan, *J. Controlled Release* **2006**, *114*, 100–9.

[24] H. Zhu, N. Shyh-Chang, A. V. Segre, G. Shinoda, S. P. Shah, W. S. Einhorn, A. Takeuchi, J. M. Engreitz, J. P. Hagan, M. G. Kharas, A. Urbach, J. E. Thornton, R. Triboulet, R. I. Gregory, D. Altshuler, G. Q. Daley, D. Consortium, M. Investigators, *Cell* **2011**, *147*, 81–94.

[25] S. T. Lee, K. Chu, H. J. Oh, W. S. Im, J. Y. Lim, S. K. Kim, C. K. Park, K. H. Jung, S. K. Lee, M. Kim, J. K. Roh, *J. Neuro-Oncol.* **2011**, *102*, 19–24.

[26] S. R. Datta, A. Brunet, M. E. Greenberg, *Gene Dev.* **1999**, *13*, 2905–2927.

[27] A. Bielen, L. Perryman, G. M. Box, M. Valenti, A. D. Brandon, V. Martins, A. Jury, S. Popov, S. Gowan, S. Jeay, F. I. Raynaud, F. Hofmann, D. Hargrave, S. A. Eccles, C. Jones, *Mol. Cancer Ther.* **2011**, *10*, 1407–1418.

[28] M. Hermisson, H. Strik, J. Rieger, J. Dichgans, R. Meyermann, M. Weller, *Neurology* **2000**, *54*, 1357–1365.

[29] A. Ito, M. Shinkai, H. Honda, K. Yoshikawa, S. Saga, T. Wakabayashi, J. Yoshida, T. Kobayashi, *Cancer Immunol. Immun.* **2003**, *52*, 80–88.

[30] F. Hirschhaeuser, H. Menne, C. Dittfeld, J. West, W. Mueller-Klieser, L. A. Kunz-Schughart, *J. Biotechnol.* **2010**, *148*, 3–15.

[31] A. C. Silva, T. R. Oliveira, J. B. Mamani, S. M. Malheiros, L. Malavolta, L. F. Pavon, T. T. Sibov, E. Amaro Jr., A. Tannús, E. L. Vidoto, M. J. Martins, R. S. Santos, L. F. Gamarra, *Int. J. Nanomed.* **2011**, *6*, 591–603.

[32] J. Zhou, T. Schmid, R. Frank, B. Brune, *J. Biol. Chem.* **2004**, *279*, 13506–13513.